Vector 3D Finite Element Method for Electromagnetic Scattering

A Project Report

submitted by

SRIRAM GOPALAKRISHNAN (EP16B005)

in partial fulfilment of requirements
for the award of the degree of

BACHELOR OF TECHNOLOGY

DEPARTMENT OF PHYSICS
INDIAN INSTITUTE OF TECHNOLOGY MADRAS

JUNE 2020

THESIS CERTIFICATE

This is to certify that the thesis titled **Vector 3D Finite Element Method for Electromagnetic Scattering**, submitted by **Sriram Gopalakrishnan**, to the Indian Institute of Technology, Madras, for the award of the degree of **Bachelor of Technology** in Engineering Physics, is a bona fide record of the research work done by him under our supervision. The contents of this thesis, in full or in parts, have not been submitted to any other Institute or University for the award of any degree or diploma.

Prof. V Sankaranarayanan
Faculty Advisor
Professor
Dept. of Physics
IIT-Madras, 600 036

Prof. Uday Khankhoje
Research Guide
Assistant Professor
Dept. of Electrical Engineering
IIT-Madras, 600 036

Place: Chennai

Date: 19th June 2020

ACKNOWLEDGEMENTS

I'm extremely thankful to my guide Dr. Uday Khankhoje for giving me this opportunity. This work draws significant inspiration from techniques taught in his graduate level course on Computational Electromagnetics. This work was done in collaboration with two other students, Siddhant Gautam and Aggraj Gupta from the Electrical Engineering department. I'm also thankful to other members of Prof. Uday's group: Chandan, Karteek, Yaswanth, and Prajosh. Discussions with all group members were enlightening. Group meetings were an excellent platform to present and learn about contemporary research in CEM.

ABSTRACT

KEYWORDS: 3D FEM, Mie scattering

We have formulated a vector-based 3D Finite Element Method (FEM) to approximate electromagnetic scattering in the Mie limit, where the wavelength of an incident plane wave is comparable to the size of a scattering dielectric object. The output of our electromagnetic FEM is a vector of electric field coefficients corresponding to edges of a tetrahedral meshing of the computational domain. In the context of RADAR remote sensing, the far-field is an important quantity, and we have formulated the far-field using Huygen's principle applied to the FEM field coefficients on the surface of the scatterer. To test the validity of the entire model computationally, we tackle the problem of Mie scattering from a homogeneous dielectric sphere, which has an analytical solution for the scattered field commonly known as the Mie Series. We have developed a custom FEM software in C++ for this purpose, however, are still in the process of perfecting the forward model to find good agreement between FEM and Mie theory.

TABLE OF CONTENTS

NOTATION

$\vec{r}$	Position vector (as a column vector unless stated otherwise)
S	Surface of scatterer
Γ	Surface of Computational Domain
Ω	Volumetric region of Computational Domain
ϵ_r	Relative permittivity (dielectric constant)
$\vec{E}$	Electric Field
$\vec{E}_{inc}$	Incident Electric Field
$\vec{E}_{scat}$	Scattered Electric Field
$\vec{H}$	Magnetic Field strength
λ	Wavelength of incident field
k_0	Free space wavevector of incident field
$L_k(x, y, z)$	Local scalar basis function of node with index $k \in \{1, 2, 3, 4\}$
$\vec{T}(x, y, z)$	Local or global vector basis function (interchangeably)
V_e	Volume of a single tetrahedral element indexed e
Δ	Area of a triangle or triangular region (context specific)
l_k	Length of an edge indexed k

CHAPTER 1

Introduction

A Finite Element Method (FEM) is an approach to find an approximate solution to a given Partial Differential Equation (PDE) in a spatial domain. It achieves this by tessellating the space into elements, which have characteristic basis functions with special properties associated with them. A linear combination of these local basis functions constitutes an approximate solution. The optimal coefficients of this linear combination are obtained by the imposition of boundary conditions and forcing functions in an application-specific formalism. Finite Element Methods are widely used in applications of Fluid Dynamics and Electromagnetics (EM).

In the context of Electromagnetics, FEMs are extensively used to study scattering from rough inhomogeneous dielectric surfaces as part of RADAR remote sensing missions. The inputs to an electromagnetic FEM are knowledge of the incident field and of the permittivity profile of the scatterer. Given these inputs, FEM gives us knowledge of the scattered (or total) field. For this reason, electromagnetic FEMs are often referred to as just "forward models". However, sensing problems in EM often involve predicting the permittivity profile of a scatterer given knowledge of the incident and scattered fields. These problems are referred to as "inverse problems", the output of which is aptly called a "reconstruction". Inverse problems are tackled in a data-driven approach using multiple iterations of a forward model. Hence, highly accurate FEMs describing the scattering behavior of a class of relevant objects are of utmost importance.

Physically, the phenomenon of a microwave scattering off a non-magnetic dielectric object is well described by classical EM in the Mie scattering limit ($\lambda \sim$ object size). In this thesis, we develop a general 3D FEM formalism to describe Mie scattering from inhomogeneous dielectrics. The problem of scattering from a homogeneous dielectric sphere is chosen to test the correctness of the forward model, since it permits an analytical solution.

CHAPTER 2

3D FEM

2.1 Problem Setting

Consider figure (2.1). We have a plane wave $\vec{E}_{inc}$ incident on a non-magnetic ($\mu_r = 1$) and in general inhomogeneous dielectric object. A homogeneous dielectric sphere is chosen only to test the theory. The object is enclosed in a computational domain, represented by the dashed lines. It is a cubical domain for the test problem. It is assumed that the wavelength of the incident field is comparable to the size of the object of interest. The wavelength is equal to the diameter of the sphere for the test problem. The surface of the scatterer is denoted S, the surface of the computational domain is denoted Γ, while its volume is denoted Ω. Given this information, we wish to approximate the scattered (or total) field at a far off point $\vec{r}\,'$. (We occasionally drop the vector symbol only to keep the analysis clean). By "far", we mean $|\vec{r}\,'|$ is much larger than the size of the object, an approximation that will become relevant in the far-field derivation. Also, the entire space is free of charges or current sources.

2.2 Weighted Residual formalism

Under the conditions stated in the previous section, the electric and magnetic fields assume a time-harmonic form with time dependence $e^{j\omega t}$. Decoupling the time dependence, the Maxwell's equations for the spatial part of the fields are given by

$$\begin{aligned} \nabla \times \vec{E} &= -j\omega\mu_0\vec{H} \\ \nabla \times \vec{H} &= j\omega\epsilon_0\epsilon_r\vec{E} \end{aligned} \tag{2.1}$$

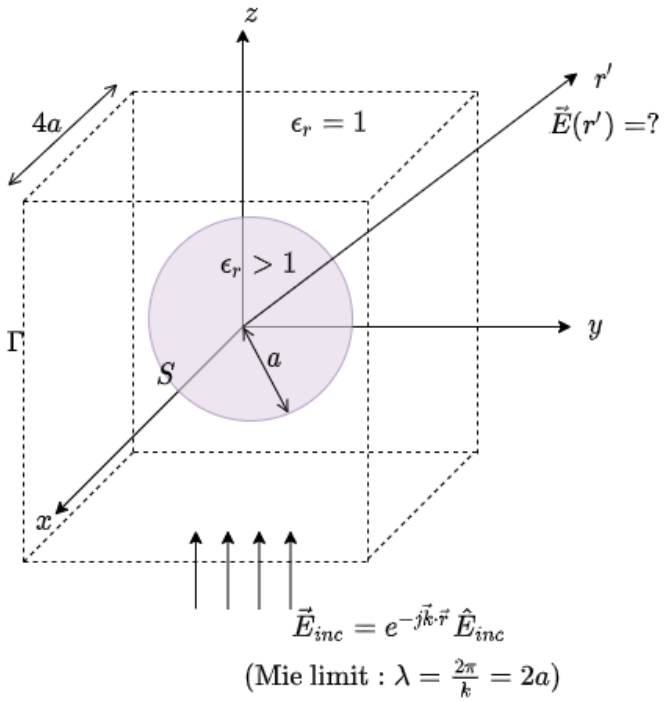

Figure 2.1: This is the physical setting of the problem we wish to test FEM against. It has a known analytical solution called Mie Series

The corresponding Helmholtz equation is given by

$$\vec{R}_E = \nabla \times (\nabla \times \vec{E}) - k_0^2 \epsilon_r \vec{E} = 0 \tag{2.2}$$

The variable $\vec{R}_E$ is called the residual and must be equal to zero for the exact solution. However, for an approximate solution $\vec{E}$ obtained from FEM, a "weighted residual" is allowed to be zero in the following manner

$$\int_\Omega \vec{T} \cdot \vec{R}_E \, dV = \int_\Omega \vec{T} \cdot \left(\nabla \times (\nabla \times \vec{E}) - k_0^2 \epsilon_r \vec{E} \right) dV = 0 \tag{2.3}$$

Here, $\vec{T}$ is a local testing function, and is also the local basis function that will be used in expressing the electric field as a linear combination. This approach of using identical testing and basis functions is called Galerkin's method. Simplifying Equation (2.3) using vector calculus identities, we get

$$\int_\Omega \left[(\nabla \times \vec{T}) \cdot (\nabla \times \vec{E}) - k_0^2 \epsilon_r \vec{T} \cdot \vec{E} \right] dV = - \oint_\Gamma \vec{T} \cdot \left(\hat{n} \times (\nabla \times \vec{E}) \right) dS \tag{2.4}$$

Here, $\hat{n}$ is the unit normal vector on the surface Γ. Note that the RHS is now a surface integral over Γ, the boundary of the computational domain. Hence, to

make any further reduction of the RHS, we first have to apply an appropriate boundary condition on the electric field. In the present case, we use a first order Absorbing Boundary Condition (ABC) as follows

$$\nabla \times \vec{E}_{scat} = -jk_0\sqrt{\epsilon_r}(\hat{n} \times \vec{E}_{scat}) \quad \text{on} \quad \Gamma \tag{2.5}$$

where $\vec{E}_{scat} = \vec{E} - \vec{E}_{inc}$ is the scattered field. Physically, this is equivalent to approximating the direction of propogation of the scattered field to be along the unit normal at the boundary. Further simplification of equation (2.4) using (2.5) yields

$$\begin{aligned} \int_\Omega \left[(\nabla \times \vec{T}) \cdot (\nabla \times \vec{E}) - k_0^2 \epsilon_r \vec{T} \cdot \vec{E}\right] dV - jk_0 \oint_\Gamma \sqrt{\epsilon_r}\vec{T} \cdot (\hat{n} \times (\hat{n} \times \vec{E}))\, dS \\ = \oint_\Gamma \left[-jk_0\sqrt{\epsilon_r}\vec{T} \cdot \Big(\hat{n} \times (\hat{n} \times \vec{E}_{inc})\Big) - \vec{T} \cdot \Big(\hat{n} \times (\nabla \times \vec{E}_{inc})\Big)\right] dS \end{aligned} \tag{2.6}$$

Notice that the RHS is now a function only of the incident field, a known quantity, while the LHS is a function of the total electric field, which we wish to approximate. Equation (2.6) is called the FEM Weak Form, and is compactly represented as

$$\Phi(\vec{T}, \vec{E}) = b(\vec{T}, \vec{E}_{inc}) \tag{2.7}$$

2.3 Galerkin Testing

Suppose there are a total of N edges in Ω after meshing. Corresponding to each global edge j is a global basis function $\vec{T}_j$ (A global edge basis function is the sum of local basis functions corresponding to each element the edge is part of). We expand the total field $\vec{E}$ in Ω in terms of the global basis functions as

$$\vec{E} = \sum_{j=1}^{N} u_j \vec{T}_j \tag{2.8}$$

There are N unknown coefficients $\{u_j\}$ to solve for. But we also have N basis functions. By setting the testing function $\vec{T}$ to each of these N basis functions, one can obtain N linear equations to solve for the coefficients. The act of using the same testing functions as the basis functions is referred to as Galerkin testing.

For $i = 1 \dots N$, we have N linear equations of the form

$$\sum_{j=1}^{N} u_j \Phi(\vec{T_i}, \vec{T_j}) = b(\vec{T_i}, \vec{E}_{inc}) \tag{2.9}$$

Hence, this can be compactly represented as $\mathbf{Au} = \mathbf{b}$, where $\mathbf{A}_{ij} = \Phi(\vec{T_i}, \vec{T_j})$, and $\mathbf{b}_i = b(\vec{T_i}, \vec{E}_{inc})$. Solving this system of equations thus gives us the the field coefficients $\{u_j\}$, and hence, knowledge of the electric field everywhere in the computational domain if the meshing is fine.

2.4 Vector tetrahedral basis functions

Until now, we have spoken about vector basis functions $\vec{T}$ without looking at their mathematical form. In this section, we define these basis functions and look at some of their special properties (Jin, 2015).

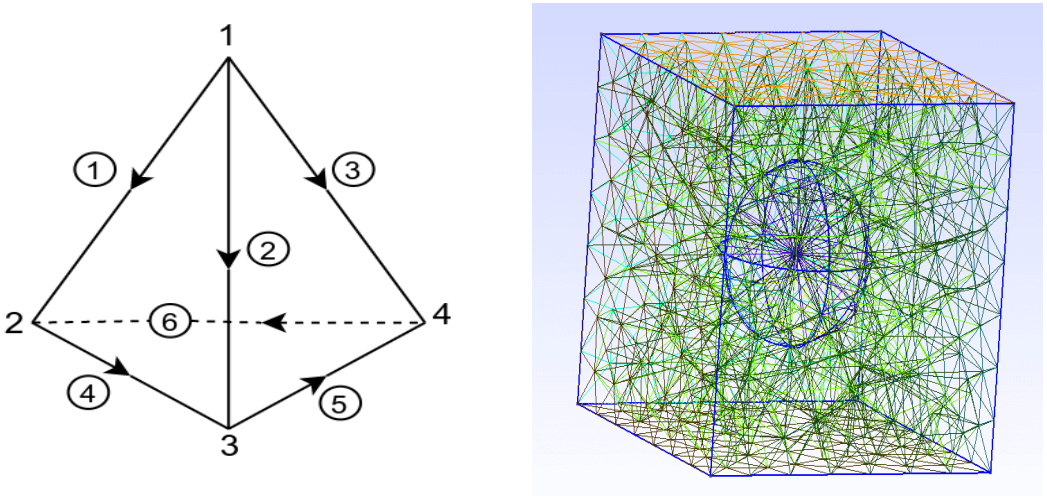

(a) Vector tetrahedral/Nedelec element: Each tetrahedron has 6 vector basis functions corresponding to 6 edges, locally numbered as shown

(b) The computational domain meshed tetrahedrally using Gmsh (Geuzaine and Remacle, 2009). A sphere is defined inside the domain

Figure 2.2

Each tetrahedral element has 6 local "edge basis functions", associated with each of the 6 edges in a special way, and can be visualized as local vector fields that are non-zero only on or inside the tetrahedral element. The functional form

of the basis function corresponding to edge k is given by

$$\vec{T}_k^e = l_k(L_{k_1}\nabla L_{k_2} - L_{k_2}\nabla L_{k_1}) \tag{2.10}$$

Here, the superscript e denotes element index e. The length of edge k is denoted l_k. Edge $k \in \{1,2,3,4,5,6\}$ is directed from node k_1 to node k_2 ($k_1, k_2 \in \{1,2,3,4\}$). Further, for each node $k \in \{1,2,3,4\}$, the scalar basis function L_k is given by

$$L_k = \frac{V_k}{V_e} := \frac{1}{6V_e}(a_k + b_k x + c_k y + d_k z) \tag{2.11}$$

Here, V_k refers to the volume of the sub-tetrahedron created by the point (x, y, z) and the triangle opposite to node k, and V_e is the volume of the whole tetrahedron. The vector tetrahedral basis function is a localized linear vector field designed to have special properties suitable for the problem at hand

- It is divergence free: $\nabla \cdot \vec{T}_1^e = 0$
- Its curl is a constant vector field: $\nabla \times \vec{T}_1^e = 2l_1(\nabla L_1 \times \nabla L_2)$
- Its component along the characteristic edge is one: for example, $\hat{e}_1 \cdot \vec{T}_1^e = 1$ (where $\hat{e}_1$ is the unit vector of edge 1 directed from node 1 to node 2)

2.5 Matrix Assembly

In section (2.3), we had arrived at a system of linear equations by abstracting integrals into the functions $\Phi(\vec{T}_i, \vec{T}_j)$ and $b(\vec{T}_i, \vec{E}_{inc})$. Here, we proceed to evaluate these integrals analytically. Simplifying equation (2.6), note that

$$\begin{aligned} A_{ij} &= \Phi(\vec{T}_i, \vec{T}_j) \\ &= \int_\Omega \left[(\nabla \times \vec{T}_i) \cdot (\nabla \times \vec{T}_j) - k_0^2 \epsilon_r \vec{T}_i \cdot \vec{T}_j\right] dV + jk_0 \oint_\Gamma \left[\sqrt{\epsilon_r}\vec{T}_i \cdot \vec{T}_j - \sqrt{\epsilon_r}(\vec{T}_i \cdot \hat{n})(\vec{T}_j \cdot \hat{n})\right] dS \\ &\equiv [P_{ij} - Q_{ij}] + [R_{ij} - S_{ij}] \end{aligned} \tag{2.12}$$

where we denote the volume integrals by P_{ij} and Q_{ij} respectively, and the surface integrals by R_{ij} and S_{ij} respectively. An important point to be noted here is that i and j are global edge indices running from 1 to N, so A_{ij} is an $N \times N$ matrix.

However, we evaluate these integrals using local basis functions, with local edge indices k and m belonging to $\{1, 2, 3, 4, 5, 6\}$. So A_{km} is a 6×6 matrix unique to each element. These local matrices are then "smeared" onto a global $N \times N$ matrix using a local to global edge mapping obtained using information in the mesh file of the computational domain.

We explicitly evaluated the integrals in equation (2.12) analytically, and present the results (including intermediate variables) directly here. (Calculation details have been documented separately, and can be made available upon request. It has been excluded in this report to limit equation redundancies)

2.5.1 Matrix P

$$P_{km} = \int_{\Omega} (\nabla \times \vec{T}_k) \cdot (\nabla \times \vec{T}_m) dV \tag{2.13}$$

Since $\vec{T}_k, \vec{T}_m$ are local, the domain of integration reduces to a single element that share these edges (k and m). We find that

$$\begin{aligned} P_{km} = \frac{l_k l_m}{324 V_e^3} \Big[& (c_{k_1} d_{k_2} - c_{k_2} d_{k_1})(c_{m_1} d_{m_2} - c_{m_2} d_{m_1}) \\ & + (d_{k_1} b_{k_2} - d_{k_2} b_{k_1})(d_{m_1} b_{m_2} - d_{m_2} b_{m_1}) \\ & + (b_{k_1} c_{k_2} - b_{k_2} c_{k_1})(b_{m_1} c_{m_2} - b_{m_2} c_{m_1}) \Big] \end{aligned} \tag{2.14}$$

2.5.2 Matrix Q

$$Q_{km} = k_0^2 \int_{\Omega} \epsilon_r \vec{T}_k \cdot \vec{T}_m dV \tag{2.15}$$

Again, the domain of integration reduces from Ω to a single element having edges k and m. We find that

$$Q_{km} = k_0^2 \, \frac{l_k l_m \epsilon_r}{36 V_e^2} \Big[I(k_1, m_1)\theta_{k_2 m_2} + I(k_2, m_2)\theta_{k_1 m_1} - I(k_1, m_2)\theta_{k_2 m_1} - I(k_2, m_1)\theta_{k_1 m_2} \Big] \tag{2.16}$$

where

$$\theta_{km} := b_k b_m + c_k c_m + d_k d_m \qquad k, m \in \{1, 2, 3, 4\} \tag{2.17}$$

and a **two-node** integral $I(k,m)$ is given by

$$I(k,m) := |J|\Bigg(\frac{n_k n_m}{6} + \frac{1}{24}\Big[n_k(f_m+g_m+h_m) + n_m(f_k+g_k+h_k)\Big] + \frac{1}{60}\Big[f_k f_m + g_k g_m + h_k h_m\Big] + \frac{1}{120}\Big[f_k(g_m+h_m) + f_m(g_k+h_k) + (g_k h_m + g_m h_k)\Big]\Bigg) \tag{2.18}$$

Within $I(k,m)$, we have a Jacobian determinant $|J|$

$$|J| = \Big|(\vec{r}_2 - \vec{r}_1) \quad (\vec{r}_3 - \vec{r}_1) \quad (\vec{r}_4 - \vec{r}_1)\Big| \tag{2.19}$$

(where $\{\vec{r}_1, \vec{r}_2, \vec{r}_3, \vec{r}_4\}$ are the position vectors of the nodes of the element in which $\vec{T}_k$ and $\vec{T}_m$ are non-zero), and intermediate variables $\{n_k, f_k, g_k, h_k\}$ defined as

$$n_k := L_k(\vec{r}_1) \quad f_k := L_k(\vec{r}_2) - L_k(\vec{r}_1) \quad g_k := L_k(\vec{r}_3) - L_k(\vec{r}_1) \quad h_k := L_k(\vec{r}_4) - L_k(\vec{r}_1) \tag{2.20}$$

And L_k is the already defined scalar basis function of node k in the element of interest.

2.5.3 Matrix R

$$R_{km} = jk_0 \oint_\Gamma \sqrt{\epsilon_r}\ \vec{T}_k \cdot \vec{T}_m\ dS \tag{2.21}$$

This time, we have a surface integral, whose domain of integration reduces from Γ to the exposed triangle (Δ) of a surface element that contain edges k and m. We find that

$$R_{km} = jk_0\ \frac{l_k l_m \sqrt{\epsilon_r}}{36 V_e^2}\Big[B(k_1,m_1)\theta_{k_2m_2} + B(k_2,m_2)\theta_{k_1m_1} - B(k_1,m_2)\theta_{k_2m_1} - B(k_2,m_1)\theta_{k_1m_2}\Big] \tag{2.22}$$

where θ_{km} is defined the same way as in the previous section, while the two-node integral $B(k,m)$ is given by

$$B(k,m) := \Delta\left[p_k p_m + \frac{1}{3}\Big(p_k(q_m+r_m) + p_m(q_k+r_k)\Big) + \frac{1}{6}(q_k q_m + r_k r_m) + \frac{1}{12}(q_k r_m + q_m r_k)\right] \tag{2.23}$$

Here, Δ is the area of the exposed triangle (with vertices $\vec{r}_1, \vec{r}_2, \vec{r}_3$) of the surface element in which edges k, m are defined, and intermediate variables $\{p_k, q_k, r_k\}$ for

$k \in \{1, 2, 3, 4\}$ are defined as

$$p_k := L_k(\vec{r}_1) \qquad q_k := L_k(\vec{r}_2) - L_k(\vec{r}_1) \qquad r_k := L_k(\vec{r}_3) - L_k(\vec{r}_1) \tag{2.24}$$

2.5.4 Matrix S

$$S_{km} = jk_0 \int_\Gamma \sqrt{\epsilon_r}(\vec{T}_k \cdot \hat{n})(\vec{T}_m \cdot \hat{n})\, dS \tag{2.25}$$

Again, the domain of integration reduces from Γ to Δ. We find that

$$S_{km} = jk_0 \, \frac{l_k l_m \sqrt{\epsilon_r}}{1296 V_e^4} \zeta(k, m) \tag{2.26}$$

where the two-node integral $\zeta(k, m)$ is given by

$$\zeta(k,m) := \Delta \left[u_k u_m + \frac{1}{3}\Big(u_k(v_m + w_m) + u_m(v_k + w_k) \Big) + \frac{1}{6}(v_k v_m + w_k w_m) + \frac{1}{12}(v_k w_m + v_m w_k) \right] \tag{2.27}$$

Δ is the area of the exposed triangle, and intermediate variables $\{u_k, v_k, w_k\}$ for $k \in \{1, 2, 3, 4\}$ are defined as

$$u_k := F_k(\vec{r}_1) \qquad v_k := F_k(\vec{r}_2) - F_k(\vec{r}_1) \qquad w_k := F_k(\vec{r}_3) - F_k(\vec{r}_1) \tag{2.28}$$

where

$$F_k(x,y,z) := \Big[(a_{k_1}\Psi_{k_2} - a_{k_2}\Psi_{k_1}) + (b_{k_1}\Psi_{k_2} - b_{k_2}\Psi_{k_1})x + (c_{k_1}\Psi_{k_2} - c_{k_2}\Psi_{k_1})y + (d_{k_1}\Psi_{k_2} - d_{k_2}\Psi_{k_1})z \Big] \tag{2.29}$$

Within this, an intermediate variable Ψ_k ($k \in \{1, 2, 3, 4\}$) is defined as

$$\Psi_k := b_k n_x + c_k n_y + d_k n_z \tag{2.30}$$

where n_x, n_y, n_z are the components of the unit normal vector at the exposed triangle of the surface element in interest.

2.5.5 Vector b

Recall from equation (2.6) that $b(\vec{T}, \vec{E}_{inc})$ is defined as

$$b(\vec{T}, \vec{E}_{inc}) = \oint_{\Gamma} \left[-jk_0\sqrt{\epsilon_r}\vec{T} \cdot \left(\hat{n} \times (\hat{n} \times \vec{E}_{inc}) \right) - \vec{T} \cdot \left(\hat{n} \times (\nabla \times \vec{E}_{inc}) \right) \right] dS \tag{2.31}$$

And the incident field vector $\mathbf{b}_i = b(\vec{T}_i, \vec{E}_{inc})$. Here, $\vec{E}_{inc}$ is an incident plane wave of the form

$$\vec{E}_{inc} = e^{-j\vec{k}_0 \cdot \vec{r}} \hat{E}_{inc} \tag{2.32}$$

Again, note that the domain of surface integration reduces from Γ to the exposed triangle Δ of the surface element $\vec{T}$ is part of. To make progress on the equation (2.31), we used a centroid approximation: if the meshing is sufficiently fine, the integral is nearly equal to the value of the integrand at the centroid of Δ times the area of Δ. Using the centroid approximation along with further reduction of the integral using the incident field (2.32), we have

$$b(\vec{T}) \approx \Delta \; jk_0 \; e^{-j\vec{k}_0 \cdot \vec{r}_G} \left[(\vec{T}(\vec{r}_G) \cdot \hat{E}_{inc}) \left(\sqrt{\epsilon_r} - (\hat{k}_0 \cdot \hat{n}) \right) - (\hat{n} \cdot \hat{E}_{inc}) \left(\vec{T}(\vec{r}_G) \cdot (\sqrt{\epsilon_r}\hat{n} - \hat{k}_0) \right) \right] \tag{2.33}$$

Here $\vec{r}_G = (\vec{r}_1 + \vec{r}_2 + \vec{r}_3)/3$ is the position vector of the centroid of Δ. Equation (2.33) was further reduced to aid programming it.

We have thus explicitly constructed the $N \times N$ FEM matrix $\mathbf{A} = (\mathbf{P} - \mathbf{Q} + \mathbf{R} - \mathbf{S})$ and the incident field vector $\mathbf{b}$, which allows us to solve $\mathbf{Au} = \mathbf{b}$ computationally so as to obtain the electric field coefficients $\{u_j\}$ everywhere in the computational domain Ω. The spatial electric field everywhere inside Ω, in the FEM approximation, is then given by $\vec{E}(\vec{r}) = \sum_j u_j \vec{T}_j(\vec{r})$.

An elegant aspect of FEM is that the matrix $\mathbf{A}$ is Sparse Band Matrix, since edges that couple must belong to the same tetrahedral element due to the local nature of the basis functions. This sparsity allows for computationally efficient matrix inversion to determine $\mathbf{u} = \mathbf{A}^{-1}\mathbf{b}$ even for fine meshing.

CHAPTER 3

Far field using Huygen's principle

Now that we have the electric field both on and inside the computational domain encoded in the field coefficients $\{u_j\}$, we wish to determine the electric field at a far off point $\vec{r}\,'$ outside the computational domain. To do so, we use the mathematical form of Huygen's principle (Sarabandi, 2009; Novotny and Hecht, 2012), that effectively "propogates" the field created by secondary point sources on the surface of the scatterer to the far-field point. So along with knowledge of the tangential fields on the scatterer surface (as obtained from FEM), we require knowledge of the free space Dyadic Green's function $\overleftrightarrow{G}(r, r')$ [1]. The reason we require a dyadic (rank-2 tensor/matrix) functional form for the Green's function is because we are dealing directly with the vector wave equation. Since both the incident and scattered fields have 3 components, the Green's function must have the form of a 3×3 matrix to effect a valid transformation.

We interpret the incident field as being generated by a vector valued current source $\vec{J}$ located far away from the scatterer, so that

$$\vec{E}_{inc}(r) \equiv \pm j\omega\mu_0 \int \overleftrightarrow{G}(r, r')\vec{J}(r')dr' \tag{3.1}$$

We may define $\vec{Q}(r) := j\omega\mu_0\vec{J}(r)$, so that the vector Helmholtz equation for the electric field in the region outside the scatterer takes the form

$$\nabla \times (\nabla \times \vec{E}) - k^2\vec{E} = \vec{Q}(r) \tag{3.2}$$

The free space dyadic Green's function $\overleftrightarrow{G}(r, r')$ thus satisfies

$$\nabla \times (\nabla \times \overleftrightarrow{G}) - k^2\overleftrightarrow{G} = \overleftrightarrow{I}\delta(r - r') \tag{3.3}$$

Take a dot product of Equation (3.2) with $\overleftrightarrow{G}$ and Equation (3.3) with $\vec{E}$, subtract them, and volume integrate (over the domain outside the scatterer, denoted V_1)

[1] The vector symbol for position vectors has been dropped in this section only to keep equations clean

on both sides. The RHS would then be the scattered field. Hence, we have

$$\vec{E}_{scat}(r') = \pm \int_{V_1} \left[(\nabla \times (\nabla \times \overleftrightarrow{G})) \cdot \vec{E} - \overleftrightarrow{G} \cdot (\nabla \times (\nabla \times \vec{E})) \right] dV \tag{3.4}$$

where $\vec{E}_{scat}(r')$ is the scattered electric field at r'. Using a different version of Green's theorem, the above volume integral can be transformed to the following surface integral (over the scatterer surface, denoted R)

$$\vec{E}_{scat}(r') = \pm \oint_R \left[\overleftrightarrow{G} \cdot \hat{n} \times (\nabla \times \vec{E}) + (\nabla \times \overleftrightarrow{G}) \cdot (\hat{n} \times \vec{E}) \right] dS \tag{3.5}$$

Here, $\hat{n}$ is the unit normal vector on the surface of the scatterer. Now, from FEM, we also get the total field coefficients u_m specifically for edges belonging to surface elements. The sum index m in the following equation is only over such edges.

$$\vec{E}_{scat}(r') = \pm \sum_m u_m \oint_R \left[\overleftrightarrow{G} \cdot \hat{n} \times (\nabla \times \vec{T}_m) + (\nabla \times \overleftrightarrow{G}) \cdot (\hat{n} \times \vec{T}_m) \right] dS \tag{3.6}$$

In the far-field limit, the 3D dyadic Green's function takes the form (Sarabandi, 2009)

$$\overleftrightarrow{G}(r, r') \approx (\overleftrightarrow{I} - \hat{r}'\hat{r}') \frac{e^{-jk|r-r'|}}{4\pi|r'|} \tag{3.7}$$

Here, $\hat{r}'\hat{r}'$ represents the outer product of the unit position vector corresponding to r' with itself. The curl of the dyadic green's function is given by (Sarabandi, 2009)

$$\nabla \times \overleftrightarrow{G} = \begin{bmatrix} 0 & -\frac{\partial}{\partial z} & \frac{\partial}{\partial y} \\ \frac{\partial}{\partial z} & 0 & -\frac{\partial}{\partial x} \\ -\frac{\partial}{\partial y} & \frac{\partial}{\partial x} & 0 \end{bmatrix} \frac{e^{-jk|r-r'|}}{4\pi|r'|} \tag{3.8}$$

Simplifying Equation (3.8) in the far-field approximation, we get

$$\nabla \times \overleftrightarrow{G} \approx \begin{bmatrix} 0 & -z' & y' \\ z' & 0 & -x' \\ -y' & x' & 0 \end{bmatrix} \frac{jk}{4\pi|r'|^2} e^{-jk|r-r'|} \tag{3.9}$$

The curl of our vector basis function is given by

$$\nabla \times \vec{T} = \frac{l}{18V^2}(c_1d_2 - c_2d_1, d_1b_2 - d_2b_1, b_1c_2 - b_2c_1) := \frac{l}{18V^2}(\beta_1, \beta_2, \beta_3) \tag{3.10}$$

Then

$$\hat{n} \times (\nabla \times \vec{T}) = \frac{l}{18V^2} \begin{vmatrix} \hat{x} & \hat{y} & \hat{z} \\ n_x & n_y & n_z \\ \beta_1 & \beta_2 & \beta_3 \end{vmatrix} := \frac{l}{18V^2}(\alpha_1, \alpha_2, \alpha_3) \tag{3.11}$$

Using the expressions in equations (3.11) and (3.7) in the first term of the scattered field integral equation (3.6), after simplifications, we have

$$\Rightarrow \overleftrightarrow{G} \cdot \hat{n} \times (\nabla \times \vec{T}) = \frac{l}{72\pi V^2} \frac{\mathbf{M} \left|\alpha\right\rangle}{|r'|^3} e^{-jk|r-r'|} \tag{3.12}$$

where

$$\mathbf{M} := \begin{bmatrix} y'^2 + z'^2 & -x'y' & -x'z' \\ -x'y' & x'^2 + z'^2 & -y'z' \\ -x'z' & -y'z' & x'^2 + y'^2 \end{bmatrix} \qquad \left|\alpha\right\rangle := \begin{pmatrix} \alpha_1 \\ \alpha_2 \\ \alpha_3 \end{pmatrix} \tag{3.13}$$

where

$$\alpha_1 := (n_y\beta_3 - n_z\beta_2) \qquad \alpha_2 := (n_z\beta_1 - n_x\beta_3) \qquad \alpha_3 := (n_x\beta_2 - n_y\beta_1) \tag{3.14}$$

$$\beta_1 := (c_1d_2 - c_2d_1) \qquad \beta_2 := (d_1b_2 - d_2b_1) \qquad \beta_3 := (b_1c_2 - b_2c_1) \tag{3.15}$$

Now

$$\hat{n} \times \vec{T} := \frac{l}{36V^2} \begin{pmatrix} \gamma_x(r) \\ \gamma_y(r) \\ \gamma_z(r) \end{pmatrix} := \frac{l}{36V^2} \left|\gamma(r)\right\rangle \tag{3.16}$$

Using the expressions in equations (3.16) and (3.9) in the second term of the scattered field integral equation (3.6), after simplifications, we have

$$\Rightarrow (\nabla \times \overleftrightarrow{G}) \cdot (\hat{n} \times \vec{T}) = \frac{l}{144\pi V^2} \frac{jk\mathbf{N} \left|\gamma(r)\right\rangle}{|r'|^2} e^{-jk|r-r'|} \tag{3.17}$$

where

$$\mathbf{N} = \begin{bmatrix} 0 & -z' & y' \\ z' & 0 & -x' \\ -y' & x' & 0 \end{bmatrix} \qquad \left|\gamma(r)\right\rangle = \begin{pmatrix} \gamma_x(r) \\ \gamma_y(r) \\ \gamma_z(r) \end{pmatrix} \tag{3.18}$$

where

$$\begin{aligned}
\gamma_x(r) &:= 6V\Big[n_y(d_2L_1(r) - d_1L_2(r)) - n_z(c_2L_1(r) - c_1L_2(r))\Big] \\
\gamma_y(r) &:= 6V\Big[n_z(b_2L_1(r) - b_1L_2(r)) - n_x(d_2L_1(r) - d_1L_2(r))\Big] \\
\gamma_z(r) &:= 6V\Big[n_x(c_2L_1(r) - c_1L_2(r)) - n_y(b_2L_1(r) - b_1L_2(r))\Big]
\end{aligned} \tag{3.19}$$

Using the results in equations (3.12) and (3.17) in the scattered field integral equation (3.6), we finally have

$$\boxed{\vec{E}_{scat}(r') \approx \pm\frac{\exp\left(-jk_0\sqrt{\epsilon_r}|r'|\right)}{72\pi|r'|^2}\sum_m\left[\frac{u_m l_m \Delta_e}{V_e^2}\left(\frac{\mathbf{M}\left|\alpha\right\rangle_m}{|r'|} + \frac{jk_0\sqrt{\epsilon_r}}{2}\mathbf{N}\left|\gamma(r_G)\right\rangle_m\right)\right]} \tag{3.20}$$

Here Δ_e is the area of the exposed surface of a surface-element e, V_e is its volume, $r_G = (r_1 + r_2 + r_3)/3$ is the position vector of the centroid of the exposed triangle.

Equation (3.20) is a neat result. Physically, it can be interpreted as a linear superposition of the fields created by secondary point-sources located at the centroids of exposed triangles on the surface of the scatterer (a sphere in our case). Notice that there is a $1/|r'|^2$ outside. But also note that $\mathbf{M}/|r'|$ and $\mathbf{N}$ have entries that linear in the coordinates of r'. So effectively, we can interpret the result as a linear superposition of the fields created by secondary point-sources. Now that we know $\vec{E}_{scat}(r')$, the Radar Cross Section (RCS) can be calculated as

$$\sigma = \lim_{r'\to\infty} 4\pi r'^2 \frac{|\vec{E}_{scat}(r')|^2}{|\vec{E}_{inc}(r')|^2} \tag{3.21}$$

Now take a look at Figure (2.1) again, where we choose a homogeneous dielectric sphere as the scatterer. In the case when the direction of propogation of the incident field is along +z ($\hat{k} = \hat{z}$) and the wave is x-polarized ($\hat{E}_{inc} = \hat{x}$), the analytical solution for the far-field is given by the Mie Series (Bohren and Huffman, 2008)

$$\vec{E}_{scat}(r') = \sum_{n=1}^{\infty} E_n(ja_n N_{e1n}^{(3)}(r') - b_n M_{o1n}^{(3)}(r')) \tag{3.22}$$

where E_n, a_n, b_n are certain coefficients, $N_{e1n}^{(3)}(r')$ and $M_{o1n}^{(3)}(r')$ even and odd vector spherical harmonics of different kinds, but with characteristic indices 1 and n.

Further, the Scattering Cross Section is analytically given by

$$\sigma = \frac{2\pi}{k_0^2} \sum_{n=1}^{\infty} (2n+1)(|a_n|^2 + |b_n|^2) \tag{3.23}$$

Finally, FEM can claim victory if there is good agreement between the analytical and numerically obtained scattering cross-sections!

CHAPTER 4

Implementation, Remarks

We are developing a custom FEM software in C++ based on the formalism presented in this thesis. Our motivation to do so is that a working customizable 3D forward model would be immensely helpful in the group's future endeavors in Remote Sensing and other inverse scattering problems.

We use Gmsh (Geuzaine and Remacle, 2009) to tetrahedrally mesh a cubic computational domain with a sphere inside (Figure (2.2b)) for different discretizations. The exported mesh file contains information about the coordinates of each node, and the nodes belonging to each tetrahedral element. This information is read into our C++ code (for FEM) as data structures for nodes and elements. Using this knowledge, data structures for edges, and surface elements were created using efficient algorithms. The FEM matrix $\mathbf{A}$ and the Incident-field vector $\mathbf{b}$ were coded using analytical expressions derived in our formulation. Exploiting the sparsity of the FEM matrix, its inversion was programmed using the SparseLU solver available in the Eigen library of C++.

We are currently in the process of perfecting the forward model to find better agreement between FEM and Mie theory. In this pursuit, we have proposed a procedure to verify the correctness of evaluation and coding of the FEM matrix using the Method of Manufactured Solutions (Marchand and Davidson, 2011) and are working towards implementing it.

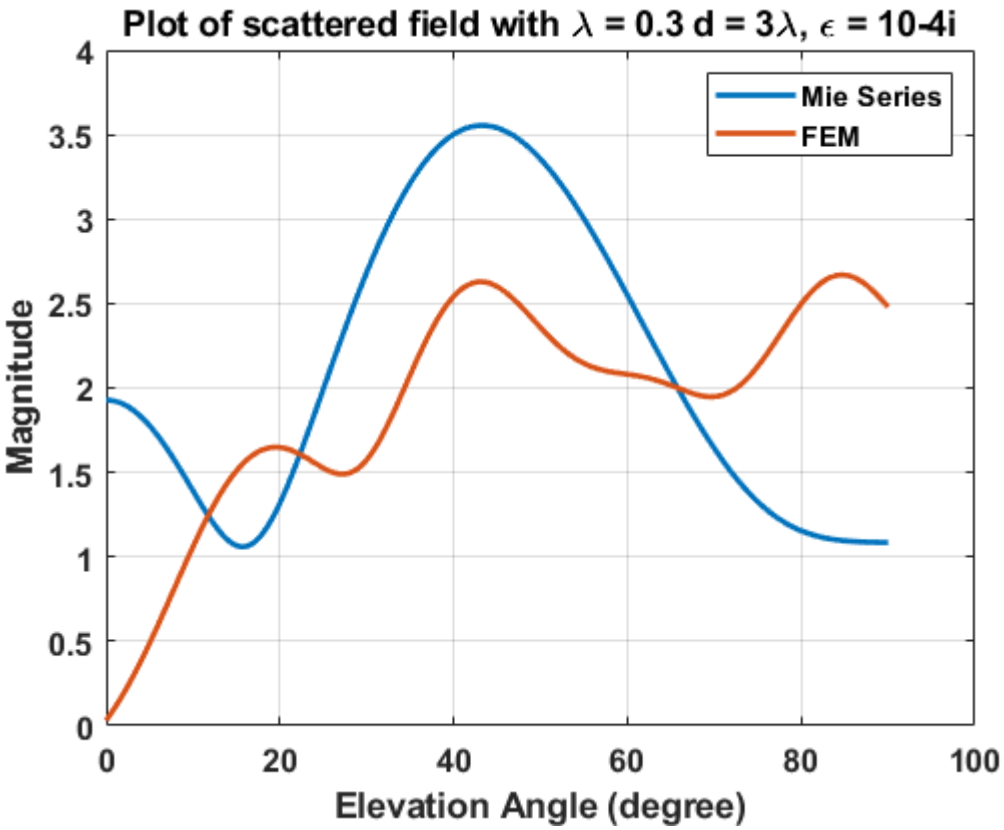

Figure 4.1: Comparison between computational and analytical far-field vs elevation angle θ: for wavelength $\lambda = 30cm$, radial distance $d = 3\lambda$, azimuth angle $\phi = 90$, complex permittivity $\epsilon = 10 - 4j$. We observe a similar nature of variations, but the agreement needs to be much stronger. We recently corrected a major flaw in our Huygen's principle formulation of far-field, which is not reflected yet in this plot

REFERENCES

1. **Bohren, C. F.** and **D. R. Huffman**, *Absorption and scattering of light by small particles*. John Wiley & Sons, 2008.

2. **Frezza, F.**, **F. Mangini**, and **N. Tedeschi** (2018). Introduction to electromagnetic scattering: tutorial. *JOSA A*, **35**(1), 163–173.

3. **Geuzaine, C.** and **J.-F. Remacle** (2009). Gmsh: A 3-d finite element mesh generator with built-in pre-and post-processing facilities. *International journal for numerical methods in engineering*, **79**(11), 1309–1331.

4. **Jin, J.-M.**, *The finite element method in electromagnetics*. John Wiley & Sons, 2015.

5. **Marchand, R.** and **D. B. Davidson**, The method of manufactured solutions for the verification of computational electromagnetics. *In 2011 International Conference on Electromagnetics in Advanced Applications*. IEEE, 2011.

6. **Novotny, L.** and **B. Hecht**, *Principles of nano-optics*. Cambridge university press, 2012.

7. **Sarabandi, K.** (2009). Dyadic Green's Function. `http://www.eecs.umich.edu/courses/eecs730/lect/DyadicGF_W09_port.pdf`.